Static and free vibration of axially loaded functionally graded beams based on the first-order shear deformation theory

Trung-Kien Nguyen[a,*], Thuc P. Vo[b], Huu-Tai Thai[c]

[a] *Faculty of Civil Engineering and Applied Mechanics, University of Technical Education Ho Chi Minh City, 1 Vo Van Ngan Street, Thu Duc District, Ho Chi Minh City, Vietnam*
[b] *School of Engineering, Glyndŵr University, Mold Road, Wrexham LL11 2AW, UK.*
[c] *Department of Civil and Environmental Engineering, Hanyang University, 17 Haengdang-dong, Seongdong-gu, Seoul 133-791, Republic of Korea.*

Abstract

The first-order shear deformation beam theory for static and free vibration of axially loaded rectangular functionally graded beams is developed. In this theory, the improved transverse shear stiffness is derived from the in-plane stress and equilibrium equation and thus, associated shear correction factor is then obtained analytically. Equations of motion are derived from the Hamilton's principle. Analytical solutions are presented for simply-supported functionally graded beams. The obtained results are compared with the existing solutions to verify the validity of the developed theory. Effects of the power-law index, material contrast and Poisson's ratio on the displacements, natural frequencies, buckling loads and load-frequency curves as well as corresponding mode shapes are investigated.

Keywords: A. Hybrid; B. Buckling; B. Vibration; C. Numerical analysis

1. Introduction

Functionally graded (FG) materials are a class of composites that have continuous variation of material properties from one surface to another and thus eliminate the stress concentration found in laminated composites. They are widely used in mechanical, aerospace, nuclear, and civil engineering. Understanding static and dynamic behaviour of FG beams is of increasing importance. For some practical applications, earlier research on the free vibration characteristics of metallic beams ([1],[2]) has shown that the effects of the axial force on natural frequencies and mode shapes are, in general, much more pronounced than those of the shear deformation and/or rotatory inertia. Many theoretical models and beam theories have been developed to solve this complicated problem. Though many works on static ([3]-[11]) and free vibration ([12]-[18]) as well as buckling analysis ([19],[20]) of FG

*Corresponding author, tel.: +848 3897 2092
Email address: ntkien@hcmute.edu.vn (Trung-Kien Nguyen)

beams are available in the open literature, only representative samples are cited here. Some researchers studied static and vibration analysis in a unified fashion ([21]-[25]). A literature survey on the subject has revealed that studies of static and free vibration of axially loaded rectangular FG beams in a unitary manner are limited. There appear to be few papers that reported on the free vibration of axially loaded FG beams with tapered and non-uniform cross-section. Shahba et al. ([26]-[28]) studied free vibration and stability of axially FG tapered Euler-Bernoulli and Timoshenko beams by using a finite element approach and by solving analytically the equations of motion. Recently, Huang et al. ([29],[30]) investigated the vibration of axially FG Timoshenko beams with non-uniform cross-section. **Although a large number of studies have been performed on linear analysis of FG beams, in these studies ([6]-[30]), the shear correction factor is assumed to be constant. In fact, this assumption is only suitable for homogeneous structures. It is no longer constant for FG plates and depends on material property distribution through their thickness ([31]). To the best of the authors' knowledge, there is no publication available that deals with the shear correction factor of rectangular FG beams and investigates the effect of improved transverse shear stiffness on their displacements, natural frequencies, buckling loads as well as load-frequency curves in the open literature. This complicated problem is not well-investigated and there is a need for further studies.**

In this paper, the first-order shear deformation beam theory (FSBT) for static and free vibration of axially loaded rectangular FG beams is developed. In this theory, the improved transverse shear stiffness is derived from the in-plane stress and equilibrium equation and thus, associated shear correction factor is then obtained analytically. Equations of motion are derived from the Hamilton's principle. Analytical solutions are presented for simply-supported FG beams. The obtained results are compared with the existing solutions to verify the validity of the developed theory. Effects of the power-law index, material contrast and Poisson's ratio on the displacements, natural frequencies, buckling loads and load-frequency curves as well as corresponding mode shapes are investigated.

2. Theoretical formulation

Consider a FG beam with length L and rectangular cross-section $b \times h$, with b being the width and h being the height. The x-, y-, and z-axes are taken along the length, width, and height of the beam, respectively, as shown in Figure 1. This FG beam is constituted by a mixture of two constituents, typically ceramic and metal located at the top and bottom surfaces of the beam, respectively. All formulations are performed under the assumption of a linear elastic behaviour and small deformations of materials. The gravity is not taken into account.

2.1. Effective material properties of FG beams

The effective material properties of FG beams are assumed to vary continuously through the beam depth by a power-law as [32]:

$$P(z) = (P_c - P_m)V_c(z) + P_m \tag{1}$$

$$V_c(z) = \left(\frac{2z+h}{2h}\right)^p \tag{2}$$

where P represents the effective material property such as Young's modulus E, Poisson's ratio ν, and mass density ρ; subscripts m and c represent the metallic and ceramic constituents, respectively; and p is the power-law index which governs the volume fraction gradation. Figure 2 illustrates the variation of the volume fraction V_c through the beam depth for various values of the power-law index p. It can be seen that the V_c varies quickly near the lowest surface for p <1 and increases quickly near the top surface for p >1.

2.2. Improved transverse shear stiffness of FG beams

The displacement field of the FSBT is given by the following expressions:

$$\begin{aligned} u(x,z) &= u_o(x) + z\theta(x) \\ w(x,z) &= w_o(x) \end{aligned} \tag{3}$$

where u_o and w_o are the axial, transverse displacement along the mid-plane of the beam and θ is rotation.

The in-plane strain and stress are in fact related by the constitutive equation:

$$\sigma_{xx}(x,z) = \bar{Q}_{11}(z)\left[\epsilon^o(x) + z\chi(x)\right] \tag{4}$$

where $\bar{Q}_{11}(z)$ is the elastic constant at location z for isotropic materials, which is defined by Young's modulus $E(z)$ and Poisson's ratio $\nu(z)$ as: $\bar{Q}_{11}(z) = E(z)/(1-\nu(z)^2)$; $\epsilon^o(x)$ and $\chi(x)$ are the axial strain and curvature of the beam, respectively. These components are related with the displacement u_o and rotation θ of the beam: $\epsilon^o(x)$=$u_{o,x}(x)$, $\chi(x)$=$\theta_{,x}(x)$, and the comma indicates partial differentiation with respect to the coordinate subscript that follows.

The generalized stress resultants (N_x, M_x) are associated with the in-plane stress σ_{xx} by the global constitutive relations:

$$\begin{aligned} N_x(x) &= A\,\epsilon^o(x) + B\,\chi(x) \\ M_x(x) &= B\,\epsilon^o(x) + D\,\chi(x) \end{aligned} \tag{5}$$

where (A, B, D) are the stiffnesses of FG beams, given by:

$$(A, B, D) = \int_{-h/2}^{h/2} (1, z, z^2) \bar{Q}_{11}(z) dz \tag{6}$$

Unlike for a homogeneous beam, which the coupling stiffness B is null, the B is present in Eq. (5) due to non-symmetrical FG beam. The in-plane strain and curvature are finally expressed by:

$$\begin{aligned} \epsilon^o(x) &= aN_x(x) + bM_x(x) \\ \chi(x) &= bN_x(x) + dM_x(x) \end{aligned} \tag{7}$$

where (a, b, d) are the components of the compliance matrix, which can be explicitly calculated in terms of $\bar{Q}_{11}(z)$. Substituting Eq. (7) into Eq. (4) leads to:

$$\sigma_{xx}(x, z) = n(z)N_x(x) + m(z)M_x(x) \tag{8}$$

where $n(z)$ and $m(z)$ are the localization components expressed by:

$$\begin{aligned} n(z) &= \bar{Q}_{11}(z)(a + zb) \\ m(z) &= \bar{Q}_{11}(z)(b + zd) \end{aligned} \tag{9}$$

Moreover, it is well known that the using of the constitutive equation for deriving the transverse shear stress is not realistic due to the fact that the shear strain is constant through the beam depth. Thus, the transverse shear stress should be calculated from the equilibrium equation, $\sigma_{xx,x} + \sigma_{xz,z} = 0$, leading to:

$$\sigma_{xz}(x, z) = -\int_{-h/2}^{z} \sigma_{xx,x}(x, \xi)\, d\xi \tag{10}$$

where the integration coefficient is selected to satisfy the boundary condition for the shear stress at the upper and lower faces of the beam. By substituting Eq. (8) into Eq. (10) and using the equilibrium equations of the beam ($N_{x,x} = 0$ and $M_{x,x} - Q_x = 0$), the following relationship is obtained:

$$\sigma_{xz}(x, z) = \tilde{m}(z)Q_x(x) \tag{11}$$

where

$$\tilde{m}(z) = -\int_{-h/2}^{z} m(\xi)\, d\xi = -bA_z(z) - dB_z(z) \tag{12}$$

with

$$A_z(z) = \int_{-h/2}^{z} \bar{Q}_{11}(\xi)\, d\xi, \quad B_z(z) = \int_{-h/2}^{z} \xi\, \bar{Q}_{11}(\xi)\, d\xi \tag{13}$$

Eq. (12) is obtained due to the in-plane uniform material properties of the beam ($n_{,x} = 0$ and $m_{,x} = 0$). Practically, Eq. (11) is very often used to estimate the transverse shear stress of homogeneous beams with a quadratic form of $\tilde{m}(z)$. By considering the balance of the shear deformation energy [33]

and taking into account the shear stress defined in Eq. (11), an improved transverse shear stiffness of FG beams can be expressed by:

$$H = \left(\int_{-h/2}^{h/2} \frac{\left(bA_z(z) + dB_z(z)\right)^2}{G(z)}\, dz \right)^{-1} \tag{14}$$

where $G(z) = E(z)/2[1 + \nu(z)]$ is the shear modulus at location z.

It is well-known that the beam models based on the FSBT require an appropriate shear correction factor to calculate the transverse shear force. For FG beams, this factor is usually taken the five-sixth value as homogeneous ones. However, in this paper, it can be easily obtained from the expression of the transverse shear stiffness as follows:

$$\kappa = \left(\int_{-h/2}^{h/2} G(z)\, dz \right)^{-1} \left(\int_{-h/2}^{h/2} \frac{\left(bA_z(z) + dB_z(z)\right)^2}{G(z)}\, dz \right)^{-1} \tag{15}$$

Eq. (15) shows that the shear correction factor κ depends on the effective material properties and material contrast of the FG beams.

2.3. Equations of motion

Equations of motion of the FSBT beams can be derived from Hamilton's principle as follows:

$$\begin{aligned} N_{x,x} &= I_0 \ddot{u}_o + I_1 \ddot{\theta} \\ M_{x,x} - Q_x &= I_1 \ddot{u}_o + I_2 \ddot{\theta} \\ Q_{x,x} + q + \tilde{N} &= I_0 \ddot{w}_o \end{aligned} \tag{16}$$

where the over dot indicates partial differentiation with respect to time, q denotes the loading, which is set to zero for buckling and vibration analysis and $\tilde{N} = \hat{N} w_{o,xx}$ is the applied in-plane load, respectively. The inertia terms I_0, I_1, I_2 are expressed by:

$$(I_0, I_1, I_2) = \int_{-h/2}^{h/2} (1, z, z^2) \rho(z) dz \tag{17}$$

Substitution of Eq. (5) into Eq. (16) by noticing that $Q_x = H(w_{o,x} + \theta)$, leads to the equations of motion of the FG beams:

$$(\mathbf{K}^{st} + \mathbf{K}^{g})\mathbf{U} - \mathbf{M}\ddot{\mathbf{U}} = \mathbf{Q} \tag{18}$$

where $\mathbf{U}^T$=$\{u_o,\ \theta,\ w_o\}$ is the displacement vector, $\ddot{\mathbf{U}}^T$=$\{\ddot{u}_o,\ \ddot{\theta},\ \ddot{w}_o\}$ is the acceleration vector and $\mathbf{Q}^T$=$\{0,\ 0,\ -q\}$ is the loading vector, respectively. The stiffness matrix $\mathbf{K}^{st}$, the geometric stiffness matrix $\mathbf{K}^{g}$, and the mass matrix $\mathbf{M}$ are given as follows:

$$\mathbf{K}^{st} = \begin{pmatrix} A\,\partial_{,xx} & B\,\partial_{,xx} & 0 \\ B\,\partial_{,xx} & D\,\partial_{,xx} - H & -H\,\partial_{,x} \\ 0 & H\,\partial_{,x} & H\,\partial_{,xx} \end{pmatrix}, \mathbf{K}^{g} = \begin{pmatrix} 0 & 0 & 0 \\ 0 & 0 & 0 \\ 0 & 0 & \hat{N}\,\partial_{,xx} \end{pmatrix}, \mathbf{M} = \begin{pmatrix} I_0 & I_1 & 0 \\ I_1 & I_2 & 0 \\ 0 & 0 & I_0 \end{pmatrix} \quad (19)$$

where the operator ∂ indicates the partial differentiation with respect to the coordinate subscript that follows. The system of equations Eq. (18) can be solved with required boundary conditions.

3. Analytical solution for simply-supported FG beams

The Navier solution procedure is used to obtain the analytical solutions for the simply-supported boundary conditions. For this purpose, the displacement functions are expressed as product of undetermined coefficients and known trigonometric functions to satisfy the governing equations and the conditions at $x = 0$ and $x = L$ which are given by:

$$w_o(0,t) = 0,\ w_o(L,t) = 0,\ M(0,t) = 0,\ M(L,t) = 0 \quad (20)$$

These boundary conditions allow to approximate the rotational and transverse displacements as following expansions:

$$u_o(x,t) = \sum_r^{\infty} u_r \cos\alpha x\, e^{i\omega t} \quad (21)$$

$$\theta(x,t) = \sum_r^{\infty} x_r \cos\alpha x\, e^{i\omega t} \quad (22)$$

$$w_o(x,t) = \sum_r^{\infty} w_r \sin\alpha x\, e^{i\omega t} \quad (23)$$

where ω is the natural frequency, $\sqrt{(i)}$=-1 the imaginary unit, $\alpha = r\pi/L$. The transverse load q is also expanded in Fourier series as:

$$q(x) = \sum_r^{\infty} q_r \sin\alpha x \quad (24)$$

$$q_r = \frac{2}{L}\int_0^L q(x)\,\sin\alpha x\, dx \quad (25)$$

where q_r is the load amplitude given explicitly for uniform distributed load ($q = q_o$) as follows:

$$q_r = \frac{4q_o}{r\pi} \quad \text{with} \quad r = 1,3,5,.... \quad (26)$$

Substituting the Eqs. (21)-(24) into Eq. (18) and assuming that the beam is subjected to in-plane load of form: $\hat{N} = -N_0$, and collecting the the displacements and rotation for any values of r so that $\mathbf{U}_r^T$=$\{u_r,\ x_r,\ w_r\}$ and $\mathbf{Q}_r^T$=$\{0,\ 0,\ q_r\}$, the following eigenvalue problem is obtained:

$$\left[(\mathbf{K}^{st}+\mathbf{K}^{g})-\omega^{2}\mathbf{M}\right]\,\mathbf{U}_{r}=\mathbf{Q}_{r} \tag{27}$$

where the mass matrix $\mathbf{M}$ is given in Eq. (19), while the components of the stiffness matrix $\mathbf{K}^{st}$ and $\mathbf{K}^{g}$ associated with $\mathbf{U}_r$ are explicitly given as follows:

$$\begin{aligned} &K_{11}^{st}=A\alpha^{2},\ K_{12}^{st}=B\alpha^{2},\ K_{13}^{st}=0\\ &K_{21}^{st}=K_{12}^{st},\ K_{22}^{st}=D\alpha^{2}+H,\ K_{23}^{st}=H\alpha\\ &K_{31}^{st}=0,\ K_{32}^{st}=H\alpha,\ K_{33}^{st}=H\alpha^{2} \end{aligned} \tag{28}$$

$$K_{ij}^{g}=0 \text{ except } K_{33}^{g}=-N_{0}\alpha^{2} \tag{29}$$

3.1. Static analysis

By setting the mass matrix to zero ($\mathbf{M}$=0) and neglecting the in-plane load ($\mathbf{K}^{g}$=0), the static problem can be written as:

$$\mathbf{K}^{st}\mathbf{U}_{r}=\mathbf{Q}_{r} \tag{30}$$

Closed-form solution of $\mathbf{U}_r$ for FG beams under uniform distributed load ($q=q_o$) can be easily obtained as follows:

$$u_{r}=\frac{Bq_{r}}{\bar{D}A\alpha^{3}},\ x_{r}=-\frac{q_{r}}{\bar{D}\alpha^{3}},\ w_{r}=\frac{(\bar{D}\alpha^{2}+H)q_{r}}{H\bar{D}\alpha^{4}}\quad \text{with}\,\bar{D}=D-\frac{B^{2}}{A} \tag{31}$$

3.2. Buckling analysis

By setting the loading vector to zero ($\mathbf{Q}=0$) and the mass matrix to zero ($\mathbf{M}=0$), the stability problem can be written as the following eigenvalue problem:

$$(\mathbf{K}^{st}+\mathbf{K}^{g})\mathbf{U}_{r}=0 \tag{32}$$

To obtain a nontrivial solution, the determinant of the stiffness matrix should be zero, that allows to obtain analytically the critical buckling load as follows:

$$N_{cr}=\bar{D}\left(\frac{\pi}{L}\right)^{2}\left[1-\frac{\bar{D}\left(\frac{\pi}{L}\right)^{2}}{H+\bar{D}\left(\frac{\pi}{L}\right)^{2}}\right] \tag{33}$$

3.3. Free vibration analysis

By setting the loading vector to zero ($\mathbf{Q}=0$), the dynamic equation can be expressed as the following eigenvalue problem:

$$\left[(\mathbf{K}^{st}+\mathbf{K}^{g})-\omega^{2}\mathbf{M}\right]\,\mathbf{U}_{r}=\mathbf{0} \tag{34}$$

Eq. (34) is general form for vibration of axially loaded FG beams. In order to obtain the nontrivial solution, the determinant should be zero, i.e. $|K_{ij} + K^g_{ij} - \omega^2 M_{ij}| = 0$. By solving the achieved equation, the buckling loads, natural frequencies and load-frequency interaction curves as well as corresponding mode shapes of simply-supported FG beams can be derived.

4. Numerical Examples

In this section, a number of numerical examples are analyzed for verification the accuracy of present study and investigation the displacements, stresses, critical buckling loads, natural frequencies and load-frequency curves as well as corresponding vibration mode shapes of simply-supported FG beams. Effects of the material contrast in Young's modulus, $n = E_c/E_m$, and power-law index p on static and vibration behaviour of FG beams are discussed in details. For convenience, the following non-dimensional terms are used, the vertical displacement and stresses of FG beams under the uniformly distributed load q_o:

$$\bar{w}_o = \frac{w_o h^3}{12} \frac{384 E_m}{5 q_o L^4} \tag{35}$$

$$\bar{\sigma}_{xx} = \sigma_{xx} \frac{h}{q_o L}, \quad \bar{\sigma}_{xz} = \sigma_{xz} \frac{h}{q_o L} \tag{36}$$

and the critical buckling loads, natural frequencies:

$$\bar{N}_{cr} = N_{cr} \frac{12 L^2}{E_m h^3} \tag{37}$$

$$\bar{\omega} = \frac{\omega L^2}{h} \sqrt{\frac{\rho_m}{E_m}} \tag{38}$$

as well as the relative error (%):

$$\text{Error}\,(\%) = \frac{P_c - P_m}{P_m} \times 100\% \tag{39}$$

where P_c, P_m: the displacement obtained from the present model and from that with the five-sixth shear correction factor.

4.1. Results for static analysis

For verification purpose, simply-supported FG beams with two length-to-height ratios, L/h=4 and 16, under the uniform distributed load, q_o, are studied. The following material properties are considered [9]: Aluminum (Al) in the upper surface with E_m=70GPa, $\nu_m = 0.3$ and Zirconia (ZnO_2) in the lower surface with E_c=200GPa, ν_c=0.3. The comparison of the dimensionless maximum displacement of the present model with that of Simsek [9] is reported in Table 1. Since Simsek [9] neglected Poisson's

ratio in $\bar{Q}_{11}(z)$ of the constitutive equation (Eq. (4)), the present corresponding model agrees well with his research. It seems that Simsek [9] uses the shear correction factor $\kappa = 1$. The effect of Poisson's ratio leads to a decrease of the mid-span transverse displacement. It implies that this ratio should be taken into account for accurate analysis of FG beams. The results obtained from the present model and from that with $\kappa = 5/6$ nearly coincide in Table 1, which means that the effect of the improved shear stiffness on the displacement can be neglected for this material contrast ($n = E_c/E_m$=20/7). The vertical displacements along the beam length are plotted in Figures 3 and 4. All the displacements decrease with increasing value of the power-law index. Figures 5 and 6 show the variations of axial stress $\bar{\sigma}_{xx}$, and transverse shear stress $\bar{\sigma}_{xz}$ through the beam depth. As expected, the traditional linear variation of $\bar{\sigma}_{xx}$ and the symmetric response of $\bar{\sigma}_{xz}$ are observed for homogeneous beams (full ceramic and full metal). The maximum axial stress is located inside the FG beam for $p > 1$, which is a significant difference from the homogeneous one. Thanks to the smooth variation of the material properties of the FG beam, the axial stress is not zero at the mid-plane, therefore, its neutral plane tends to move towards the lower surface. Besides, the shear stress distributions are greatly influenced by the power-law index, thus, no symmetric response can be seen for the FG beam.

The next example is the same as before except that in this case, the effect of the improved shear stiffness on the vertical displacement is studied. Unless mentioned otherwise, the metal constituent in the lower surface of FG beams in Figure 1 is always assumed to be Aluminum (E_m=70GPa) in the following examples. Variation of the shear correction factors, calculated from Eq. (15), with respect to the power-law index p and material contrast n is given in Table 2. These factors for FG beams of previous example ($n = 7/20$) are also given to confirm again the negligible effect of the improved shear stiffness on their static behaviour. As expected, the traditional shear correction factor ($\kappa = 5/6 = 0.8333$) is recovered by two special cases: $n = 1$ and $p = 0$, which corresponds to the homogeneous beam. It is clear that this factor is not constant and depends on the power-law index and material contrast of FG beam. The relative errors of the mid-span displacement, defined in Eq. (39), with respect to the material parameters (n, p) are plotted in Figure 7. They are calculated with $L/h = 4$ and n=2, 6, 10, 20, 30. The significant deviations are observed for high values of material contrast. For example, with $n = 30$ and $p = 15$, the maximum relative error is about 14.78%. The power-law index $p = 10$ is chosen to show the effect of length-to-height ratios on the mid-span displacement in Figure 8. The curves are flatter when this ratio is larger than 30, from which there is no significant error in using $\kappa = 5/6$.

4.2. Results for axial loaded vibration analysis

The comparison of the critical buckling loads of simply-supported FG beams with L/h=5 and 10 between the present model and Li and Batra [20] is reported in Table 3. FG beams made of aluminum (Al) and alumina (Al_2O_3), whose the material properties of Al are: E_m=70GPa, ν_m=0.23, and those of Al_2O_3 are: E_c=380GPa, ν_c=0.23, are used. The variation of the shear correction factors with respect to the power-law index is given in Table 2 ($n = 38/7$). Since Li and Batra [20] neglected Poisson's ratio and used $\kappa = 5/6$, the present corresponding model agrees well with their research. However, it is due to the effect of Poisson's ratio that there is a significant difference between the present solution and that of [20]. This effect tends to increase the critical buckling load. The solutions obtained from present model and from that with $\kappa = 5/6$ show difference indicating the effect of improved shear stiffness becomes important and can not neglected (Tables 2 and 3).

In view of comparison studies, the first three natural frequencies of FG beams with L/h=5 and 20 are given in Table 4 for different values of the power-law index. The following material properties of FG beams are considered [14]: E_m=70GPa, ν_m=0.3, ρ_m=2702 kg/m^3, E_c=380GPa, ν_c=0.3, ρ_c=3960 kg/m^3. It can be noticed that the fundamental natural frequencies obtained from present model, which neglects Poisson's ratio and uses $\kappa = 5/6$, are in excellent agreement with the reference solutions [14], which were also obtained from the FSBT. Due to the effect of Poisson's ratio, there are some slightly difference of second and third natural frequencies between present model and those of Thai and Vo [25], which were based on the third-order beam theory (TBT). Here one may verify the results obtained from the present study are very close to those provided in ([14], [25]). Effect of Poisson's ratio leads to increase the natural frequencies, which is the same response as observed in the buckling analysis.

To demonstrate the accuracy and validity of the present study further, the first five natural frequencies of FG beams with L/h=5 and 20 are evaluated in Tables 5 and 6. It should be noted that in this case only Young's modulus varies through the beam depth while mass density remains constant [18]: E_m=70GPa, E_c=380GPa, $\nu_m = \nu_c$=0.3, $\rho_m = \rho_c$=3800 kg/m^3. For L/h=20, it is seen from Table 6 that the natural frequencies are in good agreement with those of ([12], [18], [25]) for different values of power-law index with both FSBT and TBT. However, there are some discrepancies between the present results with those of [18] for $L/h = 5$ in Table 5, especially when the higher modes are considered. On the other hand, the present results seem to be more acceptable, which are very close to those of ([12], [25]). Through the close correlation observed between the present model and the earlier works, accuracy and adequacy of the present model is again established.

Finally, the effects of the axial force on the natural frequencies are investigated. The first three natural frequencies with and without the effect of the axial force are given in Table 7. The change of the natural frequencies due to the axial force is significant for all values of power-law index. The natural frequencies diminish as the axial force changes from tension to compression. It implies that the tension force has a stiffening effect while the compressive force has a softening effect on the natural frequencies. The vibration mode shapes for homogeneous beam ($p = 0$) and FG beam ($p = 5$) with L/h=5 under a compressive axial force ($N_0 = 0.5N_{cr}$) are illustrated in Figure 9. Relative measures of the axial, transverse displacements and rotation show that for homogeneous beam, all three mode shapes exhibit double coupled mode (transverse displacement and rotation), whereas, for FG one, they display triply coupled mode (axial, transverse displacement and rotation). The lowest three load-frequency curves for $p = 0$ and $p = 5$ are plotted in Figures 10 and 11. Characteristic of load-frequency curves is that the value of the axial force for which the natural frequency vanishes constitutes the buckling load. Thus, for $p = 5$, the first critical buckling occurs at $N_0 = 0.395$. As a result, the lowest branch vanishes when N_0 is slightly over this value. As the axial force increases, the second, third branch will also disappear when N_0 is slightly over 1.167 and 1.799, respectively. A comprehensive three dimensional interaction diagram of the natural frequencies, axial compressive force and power-law index is plotted in Figure 12. Three groups of curves are observed. The smallest group is for the first flexural mode and the larger ones are for the second and third flexural mode, respectively.

5. Conclusions

Static and free vibration of axially loaded rectangular functionally graded beams based on the first-order shear deformation theory are presented. The improved shear stiffness and associated shear correction factors are introduced. Equations of motion are derived from Hamilton's principle. Analytical solutions are obtained for simply-supported functionally graded beams. Effects of the power-law index, material contrast and Poisson's ratio on the displacements, stresses, natural frequencies, critical buckling loads and load-frequency curves as well as corresponding mode shapes are investigated. **The shear correction factor is not the same as the one of the homogeneous beam, it is a function of the power-law index, material contrast. Consequently, that leads to the differences of the displacement, natural frequency and critical buckling load between the present model and others using the five-sixth shear correction factor, especially when high material contrast is considered**. The inclusion of the Poisson's ratio effect leads to a decrease on the displacements and an increase on the natural frequencies and buckling loads. The present model is found to be appropriate and efficient in analyzing static and free vibration problem of FG beams

under a constant axial force.

6. Acknowledgements

The first author gratefully acknowledges financial support from Vietnam National Foundation for Science and Technology Development (NAFOSTED) under grant number 107.02-2012.07, and from University of Technical Education Ho Chi Minh City.

7. References

References

[1] W. P. Howson, F. W. Williams, Natural frequencies of frames with axially loaded Timoshenko Members, Journal of Sound and Vibration 26 (4) (1973) 503 – 515.

[2] F. Y. Cheng, W. H. Tseng, Dynamic matrix of Timoshenko beam columns, Journal of the Structural Division 99 (3) (1973) 527–549.

[3] B. V. Sankar, An elasticity solution for functionally graded beams, Composites Science and Technology 61 (5) (2001) 689 – 696.

[4] H. Zhu, B. V. Sankar, A Combined Fourier Series–Galerkin Method for the Analysis of Functionally Graded Beams, Journal of Applied Mechanics 71 (3) (2004) 421–424.

[5] Z. Zhong, T. Yu, Analytical solution of a cantilever functionally graded beam, Composites Science and Technology 67 (3-4) (2007) 481 – 488.

[6] R. Kadoli, K. Akhtar, N. Ganesan, Static analysis of functionally graded beams using higher order shear deformation theory, Applied Mathematical Modelling 32 (12) (2008) 2509 – 2525.

[7] M. Benatta, I. Mechab, A. Tounsi, E. A. Bedia, Static analysis of functionally graded short beams including warping and shear deformation effects, Computational Materials Science 44 (2) (2008) 765 – 773.

[8] S. Ben-Oumrane, T. Abedlouahed, M. Ismail, B. B. Mohamed, M. Mustapha, A. B. E. Abbas, A theoretical analysis of flexional bending of Al/Al2O3 S-FGM thick beams, Computational Materials Science 44 (4) (2009) 1344 – 1350.

[9] M. Simsek, Static analysis of a functionally graded beam under a uniformly distributed load by Ritz method, International Journal of Engineering and Applied Sciences 1 (3) (2009) 1–11.

[10] G. Giunta, S. Belouettar, E. Carrera, Analysis of FGM Beams by Means of Classical and Advanced Theories, Mechanics of Advanced Materials and Structures 17 (8) (2010) 622–635.

[11] M. Birsan, H. Altenbach, T. Sadowski, V. Eremeyev, D. Pietras, Deformation analysis of functionally graded beams by the direct approach, Composites Part B: Engineering 43 (3) (2012) 1315 – 1328.

[12] M. Aydogdu, V. Taskin, Free vibration analysis of functionally graded beams with simply supported edges, Materials & Design 28 (5) (2007) 1651 – 1656.

[13] S. A. Sina, H. M. Navazi, H. Haddadpour, An analytical method for free vibration analysis of functionally graded beams, Materials & Design 30 (3) (2009) 741 – 747.

[14] M. Simsek, Fundamental frequency analysis of functionally graded beams by using different higher-order beam theories, Nuclear Engineering and Design 240 (4) (2010) 697 – 705.

[15] G. Giunta, D. Crisafulli, S. Belouettar, E. Carrera, Hierarchical theories for the free vibration analysis of functionally graded beams, Composite Structures 94 (1) (2011) 68 – 74.

[16] A. E. Alshorbagy, M. Eltaher, F. Mahmoud, Free vibration characteristics of a functionally graded beam by finite element method, Applied Mathematical Modelling 35 (1) (2011) 412 – 425.

[17] N. Wattanasakulpong, B. G. Prusty, D. W. Kelly, M. Hoffman, Free vibration analysis of layered functionally graded beams with experimental validation, Materials & Design 36 (0) (2012) 182 – 190.

[18] K. K. Pradhan, S. Chakraverty, Free Vibration of Euler and Timoshenko Functionally Graded Beams by Rayleigh-Ritz Method, Composites Part B: Engineering 51 (0) (2013) 175 – 184.

[19] M. Aydogdu, Semi-inverse method for vibration and buckling of axially functionally graded beams, Journal of Reinforced Plastics and Composites 27 (7) (2008) 683–691.

[20] S.-R. Li, R. C. Batra, Relations between buckling loads of functionally graded Timoshenko and homogeneous Euler-Bernoulli beams, Composite Structures 95 (0) (2013) 5 – 9.

[21] A. Chakraborty, S. Gopalakrishnan, J. N. Reddy, A new beam finite element for the analysis of functionally graded materials, International Journal of Mechanical Sciences 45 (3) (2003) 519 – 539.

[22] S. Kapuria, M. Bhattacharyya, A. N. Kumar, Bending and free vibration response of layered functionally graded beams: A theoretical model and its experimental validation, Composite Structures 82 (3) (2008) 390 – 402.

[23] X.-F. Li, A unified approach for analyzing static and dynamic behaviors of functionally graded Timoshenko and Euler-Bernoulli beams, Journal of Sound and Vibration 318 (4-5) (2008) 1210 – 1229.

[24] X.-F. Li, B.-L. Wang, J.-C. Han, A higher-order theory for static and dynamic analyses of functionally graded beams, Archive of Applied Mechanics 80 (2010) 1197–1212.

[25] H.-T. Thai, T. P. Vo, Bending and free vibration of functionally graded beams using various higher-order shear deformation beam theories, International Journal of Mechanical Sciences 62 (1) (2012) 57–66.

[26] A. Shahba, R. Attarnejad, M. T. Marvi, S. Hajilar, Free vibration and stability analysis of axially functionally graded tapered Timoshenko beams with classical and non-classical boundary conditions, Composites Part B: Engineering 42 (4) (2011) 801 – 808.

[27] A. Shahba, R. Attarnejad, S. Hajilar, Free vibration and stability of axially functionally graded tapered Euler-Bernoulli beams, Shock and Vibration 18 (5) (2011) 683–696.

[28] A. Shahba, S. Rajasekaran, Free vibration and stability of tapered Euler-Bernoulli beams made of axially functionally graded materials, Applied Mathematical Modelling 36 (7) (2012) 3094 – 3111.

[29] Y. Huang, X.-F. Li, A new approach for free vibration of axially functionally graded beams with non-uniform cross-section, Journal of Sound and Vibration 329 (11) (2010) 2291 – 2303.

[30] Y. Huang, L.-E. Yang, Q.-Z. Luo, Free vibration of axially functionally graded Timoshenko beams with non-uniform cross-section, Composites Part B: Engineering 45 (1) (2013) 1493 – 1498.

[31] T. K. Nguyen, K. Sab, G. Bonnet, First-order shear deformation plate models for functionally graded materials, Composite Structures 83 (1) (2008) 25–36.

[32] J. N. Reddy, Mechanics of Laminated Composites Plates: Theory and Analysis, CRC Press, Boca Raton, 1997.

[33] J. M. Berthelot, Composite Materials: Mechanical Behavior and Structural Analysis, Springer, New York, 1999.

CAPTIONS OF TABLES

Table 1: Comparison of non-dimensional mid-span displacements of simply-supported FG beams with various values of power-law index p under a uniformly distributed load.

Table 2: Variation of the shear correction factors with respect to the power-law index p and material contrast n.

Table 3: Non-dimensional critical buckling loads of simply-supported FG beams.

Table 4: The first three non-dimensional natural frequencies of simply-supported FG beams.

Table 5: The first five non-dimensional natural frequencies of simply-supported FG beams with constant mass density through the beam depth ($L/h = 5$).

Table 6: The first five non-dimensional natural frequencies of simply-supported FG beams with constant mass density through the beam depth ($L/h = 20$).

Table 7: Effect of the axial force on the first three non-dimensional natural frequencies of simply-supported FG beams.

CAPTIONS OF FIGURES

Figure 1: Geometry of a functionally graded beam.

Figure 2: Variation of volume fraction V_c through the depth of a FG beam for various values of the power-law index p .

Figure 3: Non-dimensional transverse displacements along the beam length with $L/h = 4$.

Figure 4: Non-dimensional transverse displacements along the beam length with $L/h = 16$.

Figure 5: Non-dimensional axial stress distributions for various values of the power-law index p with $L/h = 4$.

Figure 6: Non-dimensional shear stress distributions for various values of the power-law index p with $L/h = 4$.

Figure 7: Relative error (%) of the maximum deflection with respect to the power-law index p with $L/h = 4$.

Figure 8: Relative error (%) of the maximum deflection with respect to the length-to-height ratio (L/h) with $p = 10$.

Figure 9: The first three mode shapes of homogeneous beam ($p = 0$, Fig. a, c, e) and FG beam ($p = 5$, Fig. b, d, f) with $L/h = 5$ under a axial compressive force ($N_0 = 0.5N_{cr}$).

Figure 10: Effect of the axial force on the first three natural frequencies with $L/h = 5$ and $p = 0$.

Figure 11: Effect of the axial force on the first three natural frequencies with $L/h = 5$ and $p = 5$.

Figure 12: Three dimensional interaction diagram between the axial compressive force and the first three natural frequencies with respect to the power-law index p with $L/h = 5$.

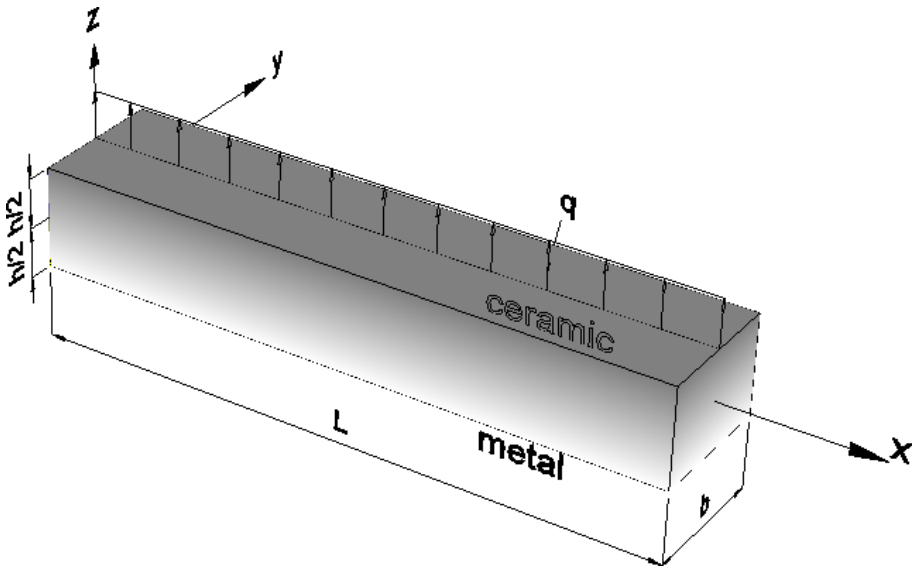

Figure 1: Geometry of a functionally graded beam.

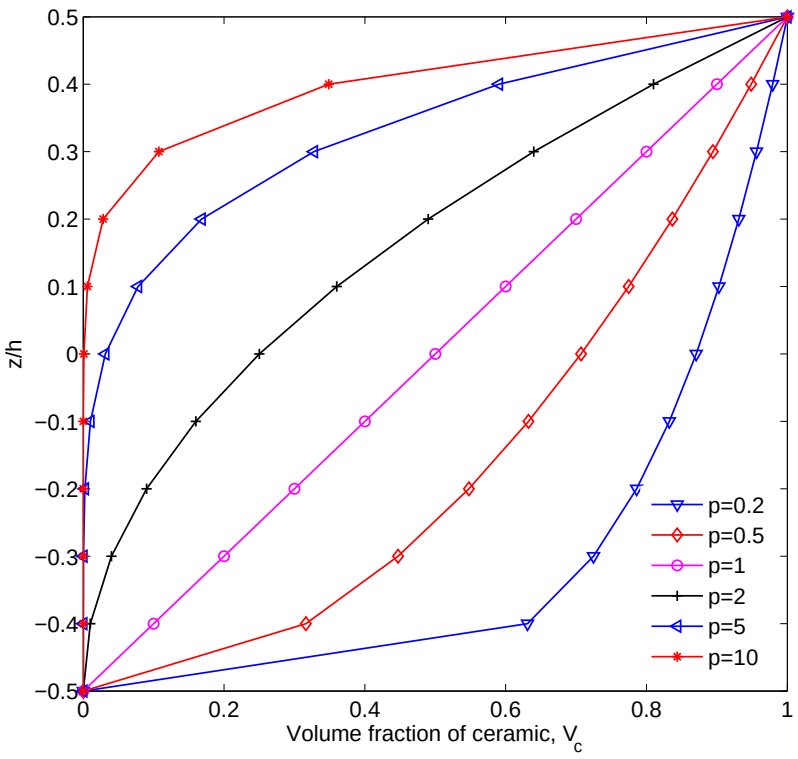

Figure 2: Variation of volume fraction V_c through the depth of a FG beam for various values of the power-law index p.

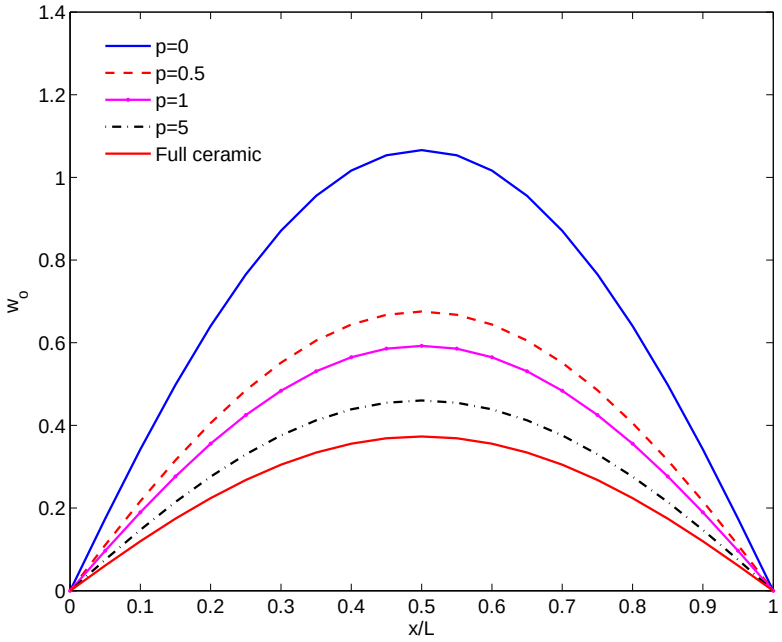

Figure 3: Non-dimensional transverse displacements along the beam length with $L/h = 4$.

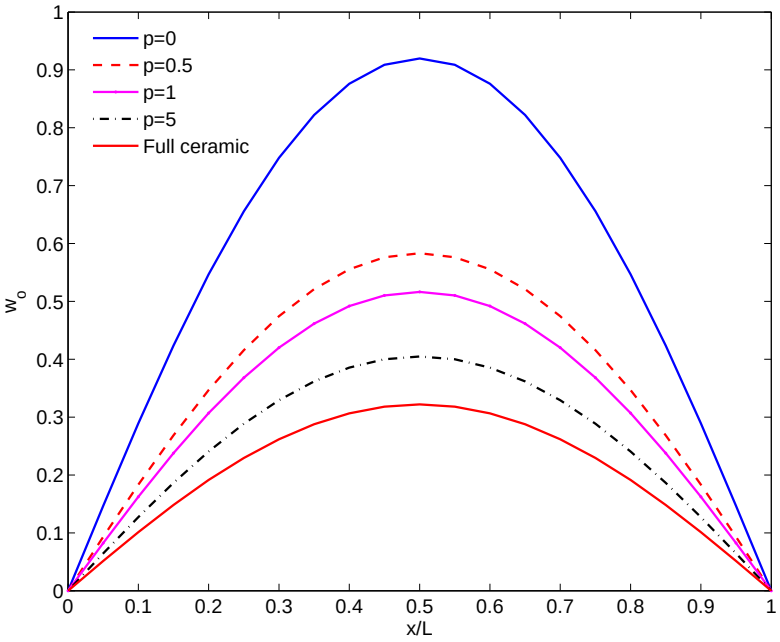

Figure 4: Non-dimensional transverse displacements along the beam length with $L/h = 16$.

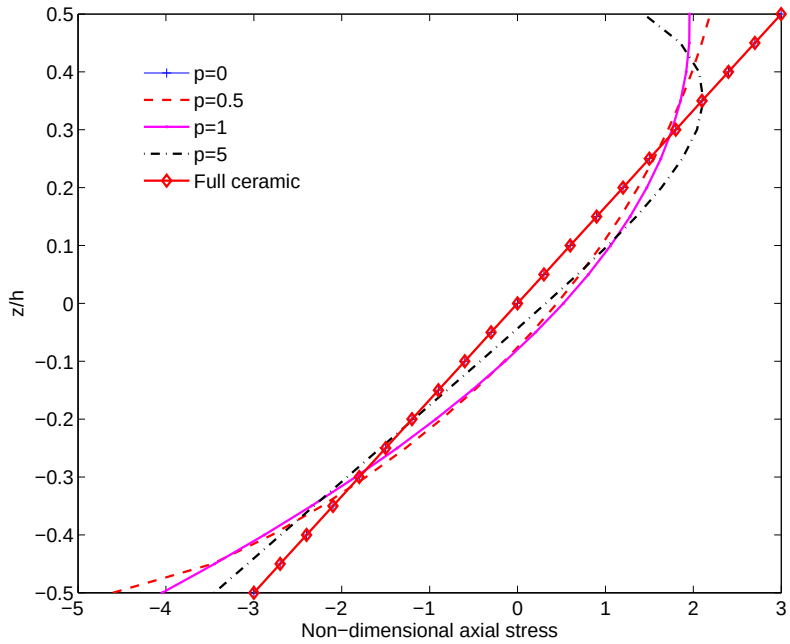

Figure 5: Non-dimensional axial stress distributions for various values of the power-law index p with $L/h = 4$.

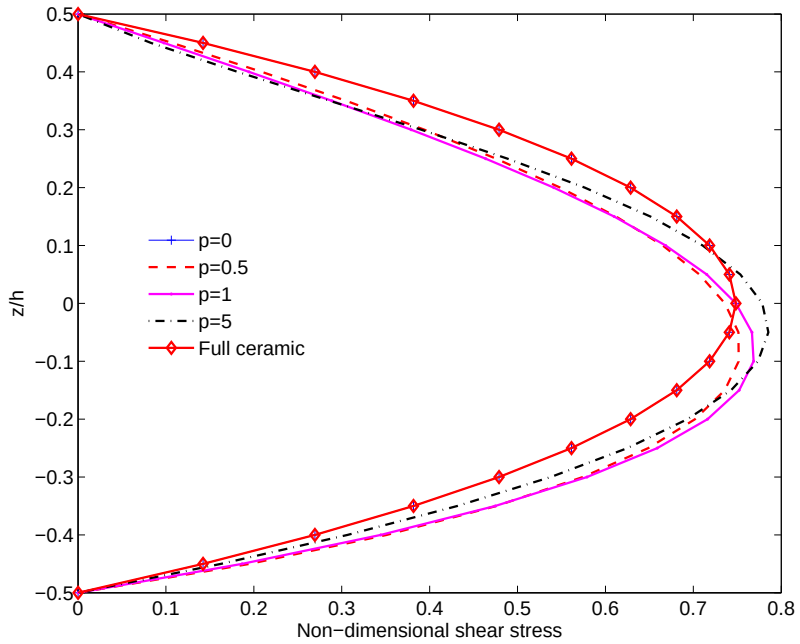

Figure 6: Non-dimensional shear stress distributions for various values of the power-law index p with $L/h = 4$.

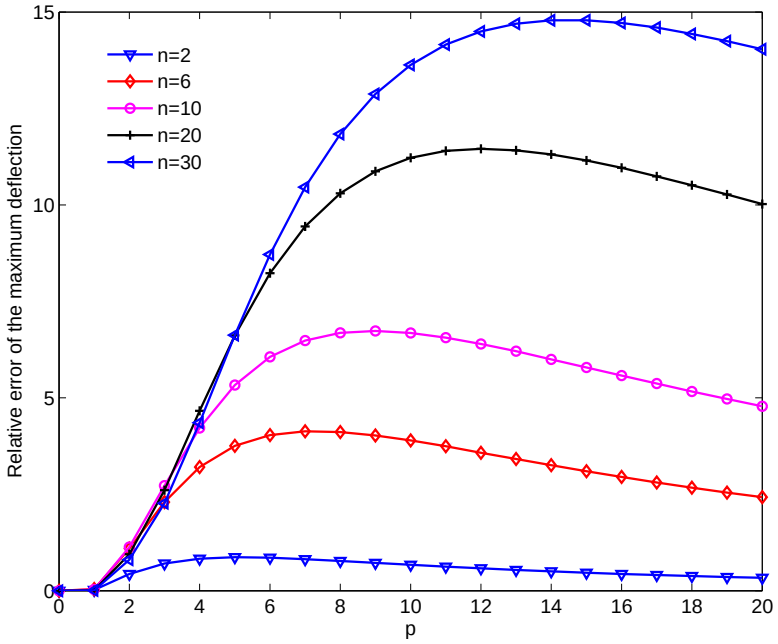

Figure 7: Relative error (%) of the maximum deflection with respect to the power-law index p with $L/h = 4$.

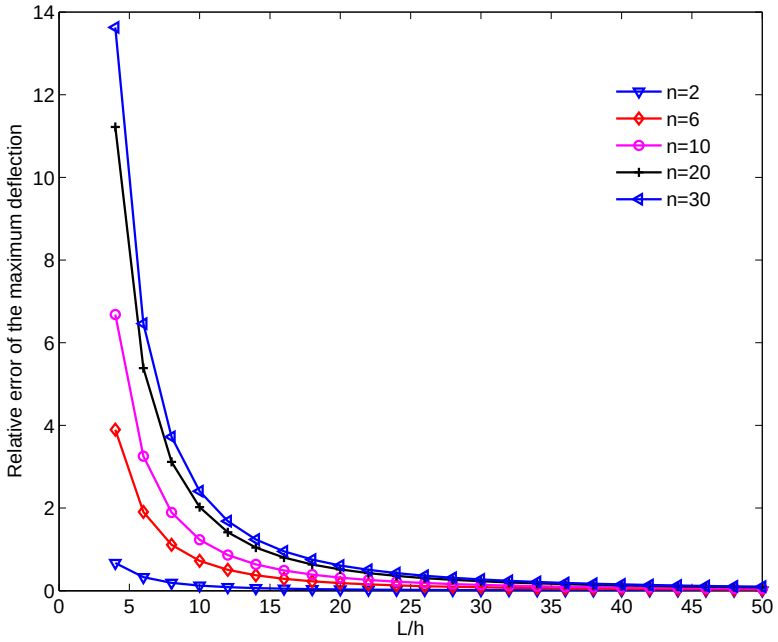

Figure 8: Relative error (%) of the maximum deflection with respect to the length-to-height ratio (L/h) with $p = 10$.

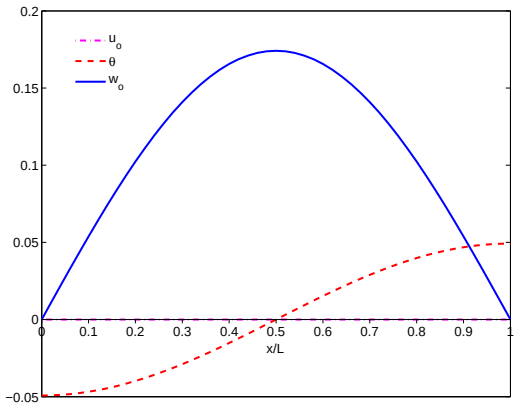

(a) Mode 1, ω_1=3.8028 with p=0

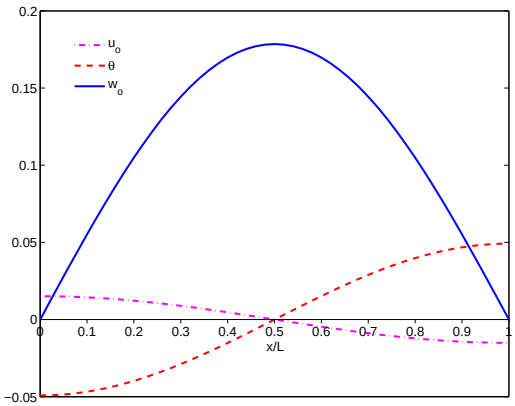

(b) Mode 1, ω_1=2.5046 with p=5

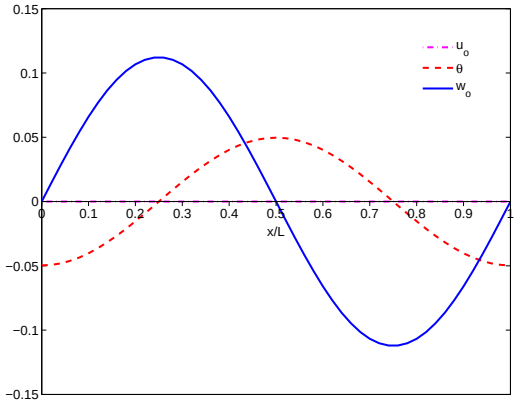

(c) Mode 2, ω_2=16.9291 with p=0

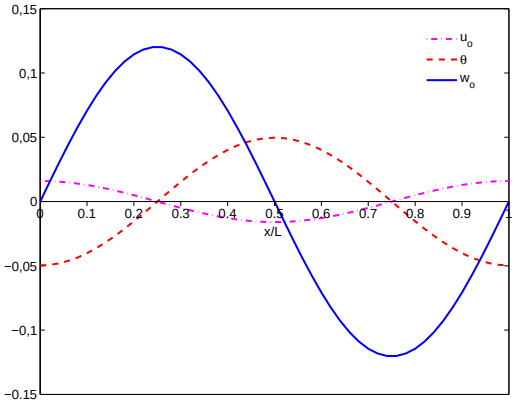

(d) Mode 2, ω_2=10.8055 with p=5

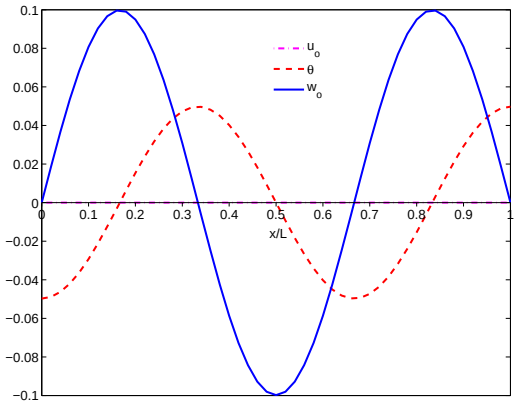

(e) Mode 3, ω_3=33.2918 with p=0

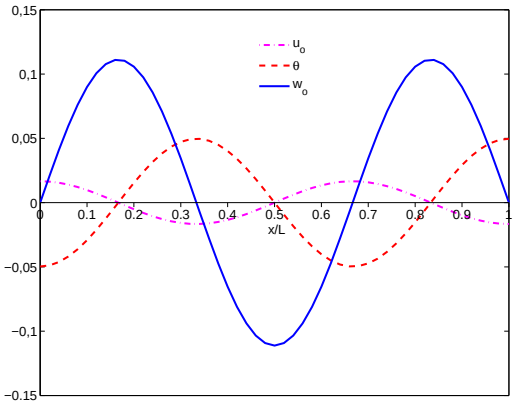

(f) Mode 3, ω_3=20.8068 with p=5

Figure 9: The first three mode shapes of homogeneous beam ($p = 0$, Fig. a, c, e) and FG beam ($p = 5$, Fig. b, d, f) with $L/h = 5$ under a axial compressive force ($N_0 = 0.5N_{cr}$).

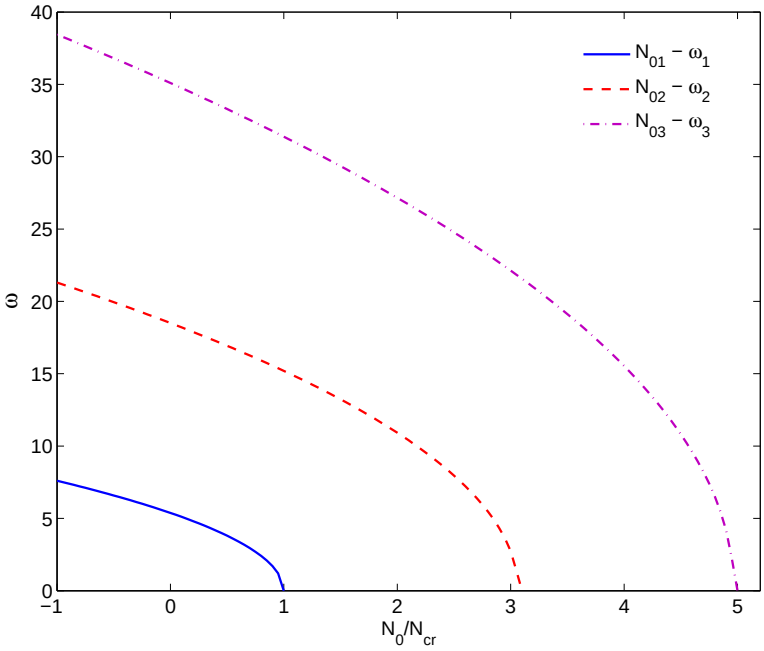

Figure 10: Effect of the axial force on the first three natural frequencies with $L/h = 5$ and $p = 0$.

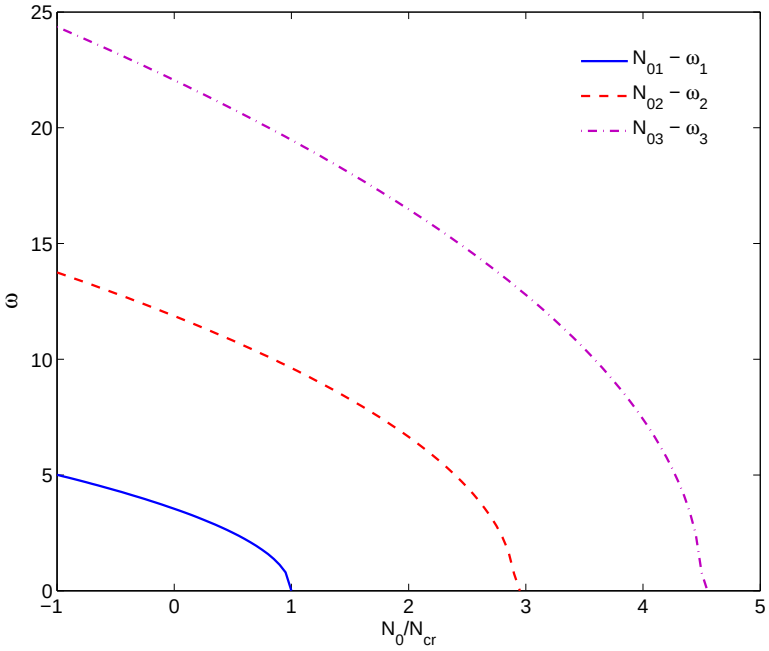

Figure 11: Effect of the axial force on the first three natural frequencies with $L/h = 5$ and $p = 5$.

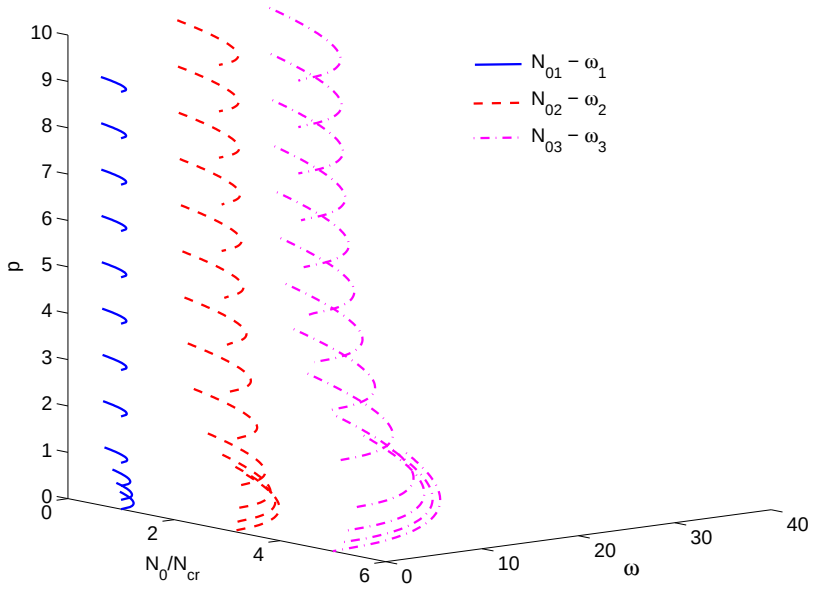

Figure 12: Three dimensional interaction diagram between the axial compressive force and the first three natural frequencies with respect to the power-law index p with $L/h = 5$.

Table 1: Comparison of non-dimensional mid-span displacements of simply-supported FG beams with various values of power-law index p under a uniformly distributed load.

L/h	Reference	p						
		0	0.2	0.5	1	2	5	Full ceramic
4	Present	1.06600	0.80283	0.67541	0.59248	0.52627	0.46024	0.37310
	Present (κ=5/6)	1.06600	0.80028	0.67337	0.59226	0.52794	0.46230	0.37310
	Present*	1.15600	0.87020	0.73248	0.64306	0.57159	0.49991	0.40460
	Present* (κ=5/6)	1.15600	0.86765	0.73044	0.64283	0.57326	0.50196	0.40460
	Present* (κ=1)	1.13000	0.84779	0.71438	0.62935	0.56164	0.49176	0.39550
	Simsek* (κ=5/6) [9]	1.13002	0.84906	0.71482	0.62936	0.56165	0.49176	0.39550
16	Present	0.91975	0.68876	0.58317	0.51644	0.46249	0.40476	0.32191
	Present (κ = 5/6)	0.91975	0.68860	0.58304	0.51642	0.46259	0.40489	0.32191
	Present*	1.00975	0.75612	0.64023	0.56701	0.50781	0.44443	0.35341
	Present* (κ = 5/6)	1.00975	0.75596	0.64011	0.56700	0.50791	0.44456	0.35341
	Present* (κ=1)	1.00812	0.75472	0.63910	0.56615	0.50718	0.44391	0.35284
	Simsek* (κ=5/6) [9]	1.00812	0.75595	0.63953	0.56615	0.50718	0.44391	0.35284

(*) : This item indicates the solution without Poisson's ratio.

Table 2: Variation of the shear correction factors with respect to the power-law index p and material contrast n

p	$n = E_c/E_m$							
	7/20	1	2	38/7	6	10	20	30
0.0	0.8333	0.8333	0.8333	0.8333	0.8333	0.8333	0.8333	0.8333
0.2	0.8180	0.8333	0.8389	0.8432	0.8437	0.8446	0.8453	0.8456
0.5	0.8177	0.8333	0.8402	0.8455	0.8458	0.8471	0.8479	0.8481
1.0	0.8310	0.8333	0.8320	0.8304	0.8305	0.8312	0.8323	0.8328
2.0	0.8538	0.8333	0.8095	0.7693	0.7662	0.7563	0.7580	0.7638
5.0	0.8622	0.8333	0.7891	0.6779	0.6641	0.5919	0.5043	0.4680
10.0	0.8507	0.8333	0.7990	0.6899	0.6746	0.5861	0.4521	0.3773

Table 3: Non-dimensional critical buckling loads of simply-supported FG beams.

L/h	Reference	p						
		0	0.2	0.5	1	2	5	10
5	Present	51.309	42.299	33.637	25.949	20.099	16.474	14.820
	Present (κ=5/6)	51.309	42.255	33.597	25.956	20.234	16.834	15.147
	Present*	48.835	40.248	31.998	24.681	19.123	15.697	14.130
	Present* (κ=5/6)	48.835	40.208	31.961	24.687	19.245	16.024	14.427
	Li and Batra* (κ=5/6) [20]	48.835	-	31.967	24.687	19.245	16.024	14.427
10	Present	55.157	45.277	35.857	27.599	21.494	18.024	16.361
	Present ($\kappa = 5/6$)	55.157	45.264	35.845	27.601	21.532	18.130	16.459
	Present*	52.308	42.935	34.000	26.169	20.382	17.098	15.524
	Present* (κ=5/6)	52.308	42.924	33.989	26.171	20.416	17.194	15.612
	Li and Batra* (κ=5/6) [20]	52.309	-	33.996	26.171	20.416	17.192	15.612

(*) : This item indicates the solution without Poisson's ratio.

Table 4: The first three non-dimensional natural frequencies of simply-supported FG beams.

L/h	Mode	Reference	p						
			0	0.2	0.5	1	2	5	10
5	1	Present	5.3778	5.0185	4.6051	4.1669	3.7828	3.5418	3.4179
		Present* (κ=5/6)	5.1525	4.8047	4.4075	3.9902	3.6344	3.4312	3.3135
		Simsek* (κ=5/6) [14]	5.1525	4.8066	4.4083	3.9902	3.6344	3.4312	3.3134
		Thai and Vo* (TBT) [25]	5.1527	-	4.4107	3.9904	3.6264	3.4012	3.2816
	2	Present	18.5019	17.3654	16.0161	14.5160	13.0562	11.8698	11.3436
		Present* (κ=5/6)	17.8711	16.7393	15.4250	14.0030	12.7120	11.8157	11.3073
		Thai and Vo* (TBT) [25]	17.8812	-	15.4588	14.0100	12.6405	11.5431	11.0240
	3	Present	35.0951	33.1059	30.6771	27.8565	24.8641	22.0568	20.9045
		Present* (κ=5/6)	34.1449	32.1098	29.7146	27.0525	24.4970	22.4642	21.3219
		Thai and Vo* (TBT) [25]	34.2097	-	29.8382	27.0979	24.3152	21.7158	20.5561
20	1	Present	5.7222	5.3244	4.8738	4.4069	4.0199	3.8228	3.7081
		Present* (κ=5/6)	5.4603	5.0805	4.6504	4.2051	3.8368	3.6509	3.5416
		Simsek* (κ=5/6) [14]	5.4603	5.0827	4.6514	4.2051	3.8368	3.6509	3.5416
		Thai and Vo* (TBT) [25]	5.4603	-	4.6511	4.2051	3.8361	3.6485	3.5390
	2	Present	22.5873	21.0309	19.2616	17.4189	15.8723	15.0404	14.5721
		Present* (κ=5/6)	21.5732	20.0824	18.3912	16.6344	15.1715	14.4110	13.9653
		Thai and Vo* (TBT) [25]	21.5732	-	18.3962	16.6344	15.1619	14.3746	13.9263
	3	Present	49.7603	46.3777	42.5121	38.4544	34.9818	32.9705	31.8869
		Present* (κ=5/6)	47.5921	44.3371	40.6335	36.7673	33.5135	31.7473	30.7176
		Thai and Vo* (TBT) [25]	47.5930	-	40.6526	36.7679	33.4689	31.5780	30.5369

(*) : This item indicates the solution without Poisson's ratio.

Table 5: The first five non-dimensional natural frequencies of simply-supported FG beams with constant mass density through the beam depth ($L/h = 5$).

Mode	Reference	p						
		0	0.2	0.5	1	2	5	10
1	Present	6.5105	5.9106	5.2676	4.6211	4.0606	3.6746	3.4893
	Present (κ=5/6)	6.5105	5.9074	5.2643	4.6217	4.0744	3.7153	3.5286
	Present (κ=1)	6.5633	5.9530	5.3025	4.6534	4.1025	3.7457	3.5611
	Aydogdu and Taskin [12]	6.5630	-	-	4.6520	4.1010	-	3.5630
	Aydogdu and Taskin (TBT) [12]	6.5740	-	-	4.6590	4.1030	-	3.5480
	Pradhan and Chakraverty [18]	6.5348	5.9659	5.4306	4.9481	4.5239	4.0732	3.7305
	Thai and Vo* (TBT) [25]	6.5109	5.9119	5.2684	4.6220	4.0648	3.6801	3.4918
2	Present	22.3986	20.4426	18.2981	16.0670	13.9871	12.3054	11.5794
	Present (κ=5/6)	22.3986	20.4112	18.2654	16.0737	14.1219	12.6812	11.9356
	Present (κ=1)	22.9266	20.8715	18.6535	16.3951	14.4024	12.9740	12.2434
	Pradhan and Chakraverty [18]	21.5695	19.6616	17.5440	15.3390	13.3481	11.9338	11.2966
	Thai and Vo* (TBT) [25]	22.4136	20.4561	18.3080	16.0830	14.0398	12.3716	11.6178
3	Present	42.4866	38.9629	35.0232	30.7946	26.6039	22.8578	21.3371
	Present (κ=5/6)	42.4866	38.8684	34.9239	30.8148	27.0059	23.9316	22.3383
	Present (κ=1)	44.0881	40.2757	36.1171	31.8018	27.8555	24.7948	23.2348
	Pradhan and Chakraverty [18]	35.9698	33.0629	29.9057	26.5843	23.3498	20.3628	18.7676
	Thai and Vo* (TBT) [25]	42.5814	39.0342	35.0780	30.8748	26.8085	23.1046	21.5015
4	Present	64.1099	59.0170	53.2414	46.8868	40.2883	34.0055	31.5443
	Present (κ=5/6)	64.1099	58.8329	53.0467	46.9264	41.0683	36.0258	33.3999
	Present (κ=1)	67.2438	61.6053	55.4099	48.8814	42.7358	37.6874	35.1070
	Pradhan[18]	38.3656	35.5499	32.2700	28.5333	24.5784	20.7687	19.0112
	Thai and Vo* (TBT) [25]	64.4193	59.2460	53.4225	47.1259	40.7960	34.5984	31.9717
5	Present	86.2022	79.5888	72.0160	63.5225	54.3772	45.2884	41.8100
	Present (κ=5/6)	86.2022	79.2985	71.7068	63.5855	55.6108	48.4044	44.6326
	Present (κ=1)	91.1638	83.7137	75.4913	66.7222	58.2705	51.0157	47.2861
	Aydogdu and Taskin [12]	91.1630	-	-	65.9460	57.4230	-	46.7160
	Aydogdu and Taskin (TBT) [12]	92.7810	-	-	67.0880	58.2300	-	46.2900
	Pradhan and Chakraverty [18]	45.3825	41.9523	38.2796	34.3969	30.3013	25.9059	23.5247
	Thai and Vo* (TBT) [25]	86.9296	80.1345	72.4565	64.0624	55.3802	46.4306	42.6755

(*) : This item is provided by Thai and Vo [25], which is not included in their paper.

Table 6: The first five non-dimensional natural frequencies of simply-supported FG beams with constant mass density through the beam depth ($L/h = 20$).

Mode	Reference	p						
		0	0.2	0.5	1	2	5	10
1	Present	6.9273	6.2727	5.5788	4.8926	4.3202	3.9682	3.7858
	Present (κ=5/6)	6.9273	6.2724	5.5786	4.8926	4.3213	3.9714	3.7890
	Present (κ=1)	6.9314	6.2759	5.5815	4.8950	4.3234	3.9738	3.7915
	Aydogdu and Taskin [12]	6.9310	-	-	4.8950	4.3230	-	3.7910
	Aydogdu and Taskin (TBT) [12]	6.9320	-	-	4.8950	4.3230	-	3.7900
	Pradhan and Chakraverty [18]	6.9317	6.3180	5.7471	5.2417	4.8112	4.3647	4.0059
	Thai and Vo* (TBT) [25]	6.9273	6.2738	5.5794	4.8926	4.3205	3.9686	3.7859
2	Present	27.3445	24.7748	22.0444	19.3339	17.0533	15.6105	14.8771
	Present (κ=5/6)	27.3445	24.7711	22.0406	19.3347	17.0696	15.6599	14.9252
	Present (κ=1)	27.4062	24.8242	22.0849	19.3714	17.1025	15.6960	14.9640
	Pradhan and Chakraverty [18]	27.4029	24.8235	22.0738	19.3446	17.0638	15.6589	14.9410
	Thai and Vo* (TBT) [25]	27.3446	24.7791	22.0469	19.3347	17.0579	15.6166	14.8795
3	Present	60.2404	54.6283	48.6420	42.6656	37.5695	34.2141	32.5540
	Present (κ=5/6)	60.2404	54.6108	48.6239	42.6692	37.6464	34.4438	32.7767
	Present (κ=1)	60.5324	54.8624	48.8344	42.8438	37.8017	34.6135	32.9584
	Pradhan and Chakraverty [18]	60.4581	54.8450	48.9315	43.1086	38.2118	34.9156	33.0512
	Thai and Vo* (TBT) [25]	60.2417	54.6387	48.6483	42.6700	37.5919	34.2437	32.5665
4	Present	104.1678	94.5697	84.2817	73.9369	64.9699	58.7933	55.8291
	Present (κ=5/6)	104.1678	94.5191	84.2294	73.9475	65.1911	59.4448	56.4580
	Present (κ=1)	105.0123	95.2484	84.8404	74.4542	65.6403	59.9313	56.9772
	Pradhan and Chakraverty [18]	104.5419	94.7983	84.2607	73.6569	64.6242	58.8679	56.1777
	Thai and Vo* (TBT) [25]	104.1743	94.5907	84.2951	73.9515	65.0375	58.8818	55.8693
5	Present	157.4895	143.1596	127.7156	112.0599	98.2418	88.2830	83.6465
	Present (κ=5/6)	157.4895	143.0485	127.6005	112.0833	98.7252	89.6864	84.9950
	Present (κ=1)	159.3471	144.6564	128.9497	113.2018	99.7131	90.7462	86.1216
	Aydogdu and Taskin [12]	159.3470	-	-	113.1700	99.6770	-	86.0890
	Aydogdu and Taskin (TBT) [12]	159.7400	-	-	113.4100	99.7490	-	85.6720
	Pradhan and Chakraverty [18]	153.4624	142.4953	127.7321	112.1508	98.8269	85.5672	77.5222
	Thai and Vo* (TBT) [25]	157.5115	143.1994	127.7422	112.0966	98.3978	88.4853	83.7456

(*) : This item is provided by Thai and Vo [25], which is not included in their paper.

Table 7: Effect of the axial force on the first three non-dimensional natural frequencies of simply-supported FG beams.

L/h	p	N_{cr}	$N_0 = -0.5N_{cr}$ (tension)			$N_0 = 0$ (no axial force)			$N_0 = 0.5N_{cr}$ (compression)		
			ω_1	ω_2	ω_3	ω_1	ω_2	ω_3	ω_1	ω_2	ω_3
5	0	1.2345	6.5864	19.9503	36.8083	5.3778	18.5019	35.0951	3.8028	16.9291	33.2918
	0.2	1.0183	6.1463	18.7075	34.6815	5.0185	17.3654	33.1059	3.5487	15.9096	31.4495
	0.5	0.8102	5.6400	17.2381	32.0996	4.6051	16.0161	30.6771	3.2564	14.6919	29.1833
	1	0.6252	5.1032	15.6152	29.1279	4.1669	14.5160	27.8565	2.9465	13.3255	26.5219
	2	0.4839	4.6327	14.0607	26.0351	3.7828	13.0562	24.8641	2.6750	11.9665	23.6325
	5	0.3955	4.3374	12.8451	23.2372	3.5418	11.8698	22.0568	2.5046	10.8055	20.8068
	10	0.3554	4.1858	12.2992	22.0770	3.4179	11.3436	20.9045	2.4169	10.2985	19.6599
	Full Metal	0.2274	3.4222	10.3660	19.1253	2.7943	9.6134	18.2351	1.9759	8.7962	17.2982
20	0	0.0853	7.0082	23.9854	51.1991	5.7222	22.5873	49.7603	4.0462	21.0968	48.2786
	0.2	0.0699	6.5210	22.3310	47.7144	5.3244	21.0309	46.3777	3.7649	19.6449	45.0014
	0.5	0.0553	5.9692	20.4510	43.7335	4.8738	19.2616	42.5121	3.4463	17.9939	41.2546
	1	0.0425	5.3973	18.4938	39.5573	4.4069	17.4189	38.4544	3.1161	16.2732	37.3189
	2	0.0332	4.9234	16.8532	35.9892	4.0199	15.8723	34.9818	2.8425	14.8266	33.9445
	5	0.0280	4.6820	15.9762	33.9367	3.8228	15.0404	32.9705	2.7031	14.0424	31.9750
	10	0.0255	4.5415	15.4812	32.8279	3.7081	14.5721	31.8869	2.6220	13.6023	30.9171
	Full Metal	0.0157	3.6414	12.4626	26.6026	2.9732	11.7362	25.8550	2.1024	10.9617	25.0852